# Analyzing the Composition and Nitrogen Isotope Concentrations of a Paleoproterozoic Era Banded Iron Formation

Amy Kingston[1,2], Hiwot Gebremedhin[1,2], Xueqi Liang[2], Daniela Gutierrez Rueda[2], Long Li[2], Daniel Alessi[2], Kurt Konhauser[2]

1 WISEST Student Researcher
2 University of Alberta, Department of Earth and Atmospheric Science

## Background

- Banded iron formations (BIF) are iron-rich and silica-rich deposits.
- The samples were collected from the Joffre Member as a part of the Hamersley Group, situated in North-West Australia.
- This formation was deposited during the Paleoproterozoic Era, which occurred around 2.5-1.6 Ga.

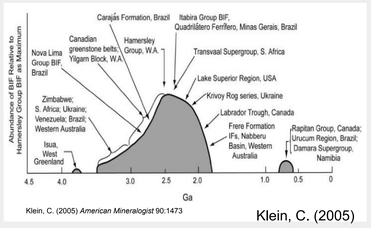


Klein, C. (2005) *American Mineralogist* 90:1473

Klein, C. (2005)

**Fig 2.** A graph showing the relationship between the size of BIFs and the approximal time of formation..

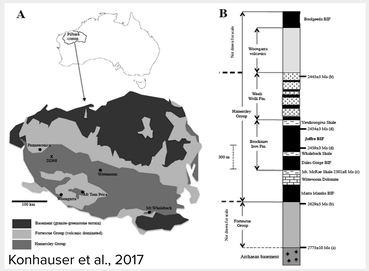


Konhauser et al., 2017

**Fig 1.** (A) The geolocation of the Hamersley group in Australia. (B) An illustration that shows the order of the BIFs and their time of deposition.

- Studying the composition and nitrogen isotope concentrations can provide a vital look into the microbial life and conditions of the oceans during the Precambrian.

## Methods

- The BIF samples, after collection, are hand ground using an agate mortar and pestle to prevent nitrogen contamination.
- Around 100mg of each sample is loaded into quartz tubes to be tested using an Isotope-Ratio Mass Spectrometer (IRMS) and a custom made ultrahigh-vacuum metal line to evaluate the stable nitrogen isotope concentrations. (Fig 3.)
- A third of the samples were loaded into crucibles and placed in a furnace at 550℃ for 4 hours then weighed to determine the loss on ignition.
- The rest of the samples were digested using $H_2O_2$, $HNO_3$, HF, and $H_3BO_3$ to remove all organics and convert the rocks into a solution.
- The digested samples are then filtered and diluted for the Inductively Coupled Plasma Mass Spectrometer (ICP-MS) to determine the rare earth element concentrations and the bulk element concentrations.

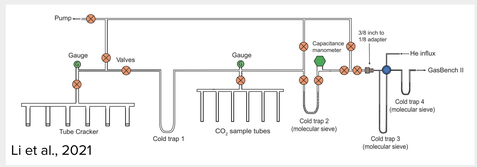


Li et al., 2021

**Fig 3.** The custom built ultrahigh-vacuum metal line located at the University of Alberta.

## Results

| Depth (m) | Sample ID | $SiO_2$ (wt%) | $Fe_2O_3$ | $Al_2O_3$ | MgO | CaO | $Na_2O$ | $K_2O$ | $MnO_2$ | $TiO_2$ | $P_2O_5$ | LOI | Total |
|---|---|---|---|---|---|---|---|---|---|---|---|---|---|
| 94.0 | DD98-1 | 23.41 | 62.94 | 0.67 | 2.07 | 0.40 | 0.20 | 0.86 | 0.05 | 0.01 | 0.03 | 3.8 | 94.47 |
| 100.7 | DD98-2 | 34.69 | 52.61 | 0.76 | 2.60 | 0.89 | 0.26 | 1.30 | 0.07 | 0.02 | 0.36 | 4.2 | 97.77 |
| 110.5 | DD98-3 | 71.57 | 29.29 | 0.12 | 1.65 | 0.11 | 2.42 | 0.13 | 0.02 | 0.01 | 0.05 | 0.7 | 106.04 |
| 120.3 | DD98-4 | 22.15 | 64.29 | 0.41 | 1.78 | 1.05 | 0.60 | 0.38 | 0.53 | 0.01 | 0.28 | 9.0 | 100.44 |
| 146.6 | DD98-7 | 50.35 | 52.90 | 0.54 | 2.07 | 0.10 | 1.59 | 0.39 | 0.02 | 0.04 | 0.03 | -0.9 | 107.16 |
| 102.2 | DD98-8 | 51.34 | 44.16 | 0.89 | 3.00 | 0.49 | 1.95 | 1.33 | 0.02 | 0.03 | 0.23 | 0.5 | 103.90 |
| 191.3 | DD98-9 | 45.84 | 56.16 | 0.65 | 1.91 | 1.46 | 0.87 | 0.48 | 0.06 | 0.01 | 0.03 | -0.3 | 107.21 |
| 197.0 | DD98-10 | 66.56 | 34.12 | 0.56 | 1.02 | 0.66 | 0.21 | 0.43 | 0.02 | 0.02 | 0.03 | 0.5 | 104.16 |
| 209.3 | DD98-15A | 70.33 | 28.40 | 0.13 | 1.13 | 0.10 | 1.62 | 0.18 | 0.06 | 0.00 | 0.03 | 1.2 | 103.15 |
| 232.8 | DD98-16-2 | 47.86 | 46.43 | 0.73 | 1.90 | 0.31 | 0.30 | 1.20 | 0.19 | 0.01 | 0.03 | 4.6 | 103.58 |
| 251.7 | DD98-19B | 46.76 | 45.74 | 0.58 | 2.13 | 1.48 | 0.36 | 0.73 | 0.41 | 0.02 | 0.04 | 5.2 | 103.44 |
| 281.6 | DD98-21 | 28.22 | 61.02 | 0.73 | 1.30 | 0.61 | 0.21 | 0.65 | 0.04 | 0.02 | 0.02 | 0.5 | 93.37 |
| 300.2 | DD98-22 | 74.21 | 22.70 | 0.22 | 0.38 | 0.08 | 0.47 | 0.22 | 0.01 | 0.00 | 0.05 | 0.0 | 98.38 |
| 310.4 | DD98-23 | 82.28 | 19.91 | 0.16 | 0.85 | 0.14 | 0.69 | 0.12 | 0.04 | 0.00 | 0.04 | 2.4 | 106.66 |
| 358.2 | DD98-24 | 33.47 | 49.69 | 1.23 | 2.44 | 1.82 | 0.40 | 0.83 | 0.56 | 0.04 | 0.28 | 11.6 | 102.32 |
| 364.3 | DD98-25 | 36.64 | 44.65 | 1.74 | 2.90 | 1.88 | 0.29 | 1.10 | 0.41 | 0.05 | 0.05 | 9.1 | 98.81 |
| 411.2 | DD98-26B | 18.65 | 74.81 | 0.18 | 1.43 | 1.11 | 0.11 | 0.14 | 0.03 | 0.00 | 0.27 | -1.5 | 95.23 |
| 430.5 | DD98-27 | 34.08 | 68.44 | 0.08 | 0.36 | 0.58 | 0.22 | 0.07 | 0.02 | 0.00 | 0.03 | -1.6 | 102.27 |
| 444.0 | DD98-29 | 48.18 | 47.01 | 0.08 | 1.61 | 0.32 | 1.81 | 0.05 | 0.00 | 0.00 | 0.10 | 0.2 | 99.34 |
| 448.5 | DD98-30 | 53.62 | 46.47 | 0.12 | 1.45 | 0.94 | 0.25 | 0.31 | 0.02 | 0.00 | 0.03 | 1.7 | 104.86 |

**Fig 4.** This chart outlines results from the ICP-MS for major element concentrations as well as the loss on ignition for each sample.

| Depth (m) | Sample ID | V (ppm) | Cr | Ni | Zn | Rb | Sr | Zr | Mo | S | Ba | Co | Be |
|---|---|---|---|---|---|---|---|---|---|---|---|---|---|
| 94.0 | DD98-1 | 5.16 | 5.48 | 8.28 | / | 75.16 | 11.29 | 10.70 | 0.40 | / | 52.26 | 1.58 | 0.86 |
| 100.7 | DD98-2 | 6.65 | 8.93 | 6.79 | 25.80 | 101.90 | 39.23 | 14.72 | 0.19 | 197.27 | 49.05 | 1.65 | 3.78 |
| 110.5 | DD98-3 | 5.75 | 10.90 | 9.20 | 22.55 | 6.35 | 1.48 | 4.82 | 2.02 | / | 22.46 | 1.28 | 1.32 |
| 120.3 | DD98-4 | 6.58 | 9.55 | 9.60 | 6.77 | 32.32 | 30.70 | 7.23 | 2.21 | / | 43.64 | 2.18 | 1.28 |
| 146.6 | DD98-7 | 36.83 | 6.59 | 8.14 | 39.31 | 21.68 | 2.12 | 8.42 | 0.48 | / | 157.79 | 3.18 | 2.55 |
| 102.2 | DD98-8 | 12.28 | 18.21 | 16.89 | 47.29 | 104.18 | 22.63 | 9.24 | 3.54 | 222.09 | 57.11 | 3.44 | 1.85 |
| 191.3 | DD98-9 | 8.23 | 10.48 | 8.15 | 18.46 | 30.61 | 35.75 | 9.90 | 0.33 | / | 19.39 | 1.96 | / |
| 197.0 | DD98-10 | 5.59 | 12.46 | 10.81 | 23.91 | 26.55 | 13.14 | 7.19 | 0.91 | / | 21.27 | 2.18 | / |
| 209.3 | DD98-15A | 3.88 | 5.89 | 7.42 | 23.31 | 12.91 | 2.49 | 1.57 | 1.15 | / | 45.01 | 0.98 | / |
| 232.8 | DD98-16-2 | 4.91 | 5.84 | 7.05 | 26.03 | 95.27 | 5.81 | 4.45 | 0.35 | / | 56.39 | 2.07 | / |
| 251.7 | DD98-19B | 5.08 | 8.15 | 8.66 | 29.79 | 56.50 | 32.82 | 6.97 | 0.20 | 237.02 | 76.21 | 1.91 | / |
| 281.6 | DD98-21 | 6.88 | 9.37 | 10.76 | / | 59.80 | 16.59 | 14.46 | 0.87 | / | 128.86 | 1.13 | 1.44 |
| 300.2 | DD98-22 | 4.05 | 9.99 | 12.87 | / | 20.10 | 12.61 | 3.75 | 1.80 | / | 52.35 | 1.28 | / |
| 310.4 | DD98-23 | 8.30 | 16.16 | 17.07 | / | 10.24 | 4.80 | 2.08 | 2.55 | / | 30.83 | 1.82 | / |
| 358.2 | DD98-24 | 10.41 | 12.11 | 9.66 | 22.54 | 44.73 | 29.96 | 13.10 | 0.78 | 753.58 | 112.95 | 3.14 | 1.42 |
| 364.3 | DD98-25 | 8.15 | 16.82 | 12.74 | 20.22 | 67.32 | 27.52 | 23.50 | 0.48 | 1301.06 | 116.96 | 4.45 | 2.21 |
| 411.2 | DD98-26B | 5.66 | 3.76 | 5.01 | 5.90 | 16.27 | 28.33 | 6.79 | 1.27 | / | 14.85 | 0.76 | / |
| 430.5 | DD98-27 | 3.16 | 9.37 | 12.38 | / | 9.34 | 16.69 | 1.84 | 1.45 | / | 26.00 | 1.37 | / |
| 444.0 | DD98-29 | 2.96 | 3.30 | 7.42 | 11.55 | 6.47 | 11.37 | 1.82 | 0.44 | / | 27.69 | 0.55 | 0.78 |
| 448.5 | DD98-30 | 6.49 | 13.24 | 13.70 | 18.51 | 52.46 | 33.90 | 3.51 | 1.19 | / | 16.77 | 1.38 | / |

**Fig 5.** This chart outline the results from the ICP-MS for trace elements.

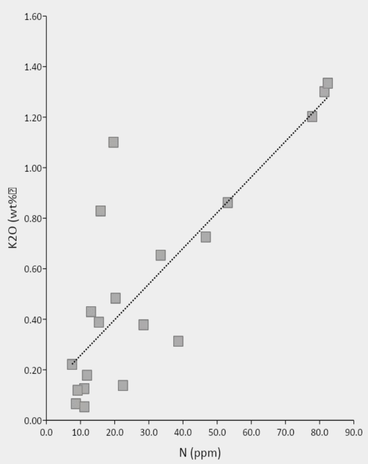


**Fig 6.** A graphical relationship between potassium concentration and nitrogen concentration because of the affinity of $NH_4^+$ to take the place of $K^+$. (Busigny et al.,2013)

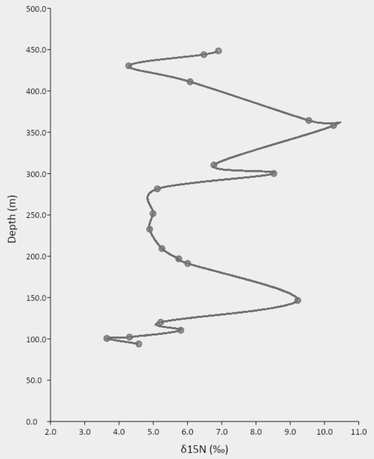


**Fig 7.** The relationship between the nitrogen isotope ratio, collected using the IRMS, and the depth the samples were collected from.

## Conclusions

- Based on Fig. 4 and Fig. 5, we can compare results to determine if the samples are from a BIF.
- Minimal detrital input during deposition is indicated by low concentrations of $Al_2O_3$ (< 1wt%) and trace elements enriched in crustal rocks (Zr, Th, and Sc < 20ppm). (Konhauser et al., 2017)
- There is also a low abundance of $TiO_2$ (< 0.04 wt%) in banded iron formations. (Haugaard et al., 2016)
- The results confirm we are dealing with a banded iron formation.
- Fig 6 resulted in a linear relationship between the N and K.
- All elements were compared to the N concentration, but only K, Rb, and Cs showed a linear correlation, where K was the most pronounced. Which means the nitrogen exists in the K bearing minerals.
- Two minerals have K: K-feldspar and stilpnomelane. (Haugaard et al., 2016)
- According to figure 8, enriched $^{15}N$ indicates a more oxidize environment and lower values indicate a reduced environment, which is indicated in Fig. 7 (Stüeken et al., 2016).

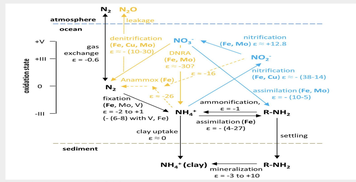


Stüeken et al., 2016

**Fig 8.** An illustration of marine nitrogen cycle. Blue marks oxic processes and orange marks suboxic processes.

## Acknowledgements

- I want to give special thanks to Katherine Snihur, as one of my main supervisors throughout my time at the University of Alberta, and the WISEST team for making this all possible.
- Thank you to Maicon Araujo for sharing his knowledge in the lab, as well as the rest of the Dr. Konhauser and Dr. Alessi lab groups.
- I would like to thank Edmonton Beta Sigma Phi and Canada Summer Jobs for their kind donations.

## References

Eva E. Stüeken, Michael A. Kipp, Matthew C. Koehler, Roger Buick, 2016. The evolution of Earth's biogeochemical nitrogen cycle. 160: 220-239 I Klein C. 2005 American Mineralogist 90:1473 I K.O. Konhauser, N.J. Planavsky, D.S. Hardisty, L.J. Robbins, T.J. Warchola, R. Haugaard, S.V. Lalonde, C.A. Partin, P.B.H. Oonk, H. Tsikos, T.W. Lyons, A. Bekker, C.M. Johnson, 2017. Iron formations: A global record of Neoarchaean to Palaeoproterozoic environmental history. 172: 140-177 I Long Li, Kan Li, Yingzhou Li, Ji Zhang, Yifan Du, Mark Labbe. 2021. Recommendations for offline combustion-based nitrogen isotopic analysis of silicate minerals and rocks. 35 (10): 1-7 I Rasmus Haugaard, Ernesto Pecoits, Stefan Lalonde, Olivier Rouxel, Kurt Konhauser, 2016. The Joffre banded iron formation, Hamersley Group, Western Australia: Assessing the paleoenvironment through detailed petrology and chemostratigraphy. 273: 12-37 I Vincent Busigny, Oanez Lebeau, Magali Ader, Bryan Krapez, Andrey Bekker, 2013. Nitrogen cycle in the Late Archean Ferruginous ocean. 362: 115-130.